INTEG. AND COMP. BIOL., 42:243–257 (2002)

Experimental Hydrodynamics of Fish Locomotion: Functional Insights from Wake Visualization[1]

ELIOT G. DRUCKER[2,*] AND GEORGE V. LAUDER†

*Department of Ecology and Evolutionary Biology, University of California, Irvine, California 92697
†Museum of Comparative Zoology, Harvard University, 26 Oxford St., Cambridge, Massachusetts 02138

SYNOPSIS. **Despite enormous progress during the last twenty years in understanding the mechanistic basis of aquatic animal propulsion—a task involving the construction of a substantial data base on patterns of fin and body kinematics and locomotor muscle function—there remains a key area in which biologists have little information: the relationship between propulsor activity and water movement in the wake. How is internal muscular force translated into external force exerted on the water? What is the pattern of fluid force production by different fish fins (*e.g.*, pectoral, caudal, dorsal) and how does swimming force vary with speed and among species? These types of questions have received considerable attention in analyses of terrestrial locomotion where force output by limbs can be measured directly with force plates. But how can forces exerted by animals moving through fluid be measured? The advent of digital particle image velocimetry (DPIV) has provided an experimental hydrodynamic approach for quantifying the locomotor forces of freely moving animals in fluids, and has resulted in significant new insights into the mechanisms of fish propulsion. In this paper we present ten "lessons learned" from the application of DPIV to problems of fish locomotion over the last five years. (1) Three-dimensional DPIV analysis is critical for reconstructing wake geometry. (2) DPIV analysis reveals the orientation of locomotor reaction forces. (3) DPIV analysis allows calculation of the magnitude of locomotor forces. (4) Swimming speed can have a major impact on wake structure. (5) DPIV can reveal interspecific differences in vortex wake morphology. (6) DPIV analysis can provide new insights into the limits to locomotor performance. (7) DPIV demonstrates the functional versatility of fish fins. (8) DPIV reveals hydrodynamic force partitioning among fins. (9) DPIV shows that wake interaction among fins may enhance thrust production. (10) Experimental hydrodynamic analysis can provide insight into the functional significance of evolutionary variation in fin design.**

INTRODUCTION

The study of animal functional morphology has as a central objective to clarify the physical mechanisms underlying organismal behavior. For most animals, stabilization and propulsion of the body during locomotion are behaviors with critical importance throughout life, playing a central role in prey capture, predator avoidance, reproduction and migration. A biomechanical approach to the study of locomotor function is ultimately concerned with the question of how propulsive forces are generated. For terrestrial animals, devices such as force plates have been used successfully to measure the forces applied by the limbs directly to the ground during locomotion (*e.g.*, Cavagna, 1975; Biewener and Full, 1992; Roberts *et al.*, 1998). For animals that move through fluids, however, such force transducers are not readily applicable, and alternative approaches are required for investigating locomotor function.

In studying the mechanics of locomotion by animals in fluids, two levels of analysis are required: musculoskeletal and hydrodynamic. At the first level, one asks how a propulsor is built and how it moves during locomotion. For swimming animals, there has been extensive study of the anatomy and kinematics of aquatic propulsors (recent work includes Geerlink, 1983; Videler, 1993; Gibb *et al.*, 1994; Drucker and Jensen, 1996; Gillis, 1996; Domenici and Blake, 1997; Long *et al.*, 1997; Walker and Westneat, 1997; Fish, 1998), as well as description of their neuromuscular control (Grillner and Wallen, 1984; Eaton *et al.*, 1988; Jayne and Lauder, 1995; Wardle *et al.*, 1995; Westneat and Walker, 1997). These data provide important information about the internal mechanisms by which swimming force may be generated. In addition, *in vitro* study of muscle physiology allows direct measurement of the mechanical forces available for propulsion (Altringham and Johnston, 1990; Luiker and Stevens, 1993; Rome *et al.*, 1993; Coughlin, 2000). Indeed, most experimental work on the question of how animals swim has employed an approach focusing on musculoskeletal mechanics.

At the second level of analysis, one asks how the propulsor influences fluid in its wake. Although analysis of internal muscular forces contributes to an overall understanding of the locomotor mechanism, ultimately these mechanical forces must be transmitted to the fluid surrounding the animal for propulsion to occur. By examining the morphology and momentum of the wake shed by swimming organisms, it is possible to estimate the external forces produced during aquatic locomotion. The complexity of unsteady fluid flow around freely swimming animals has required that hydrodynamic analyses of locomotion be largely theoretical, focusing on mathematical or computational modeling (Weihs, 1972*a*; Lighthill, 1975; Blake, 1981; Lighthill and Blake, 1990; Fauci, 1996; Liu *et al.*,

[1] From the symposium *Molecules, Muscles, and Macroevolution: Integrative Functional Morphology* presented at the Annual Meeting of the Society for Integrative and Comparative Biology, 3–7 January 2001, at Chicago, Illinois.

[2] E-mail: edrucker@uci.edu

1997; Carling *et al.*, 1998; Walker and Westneat, 2000).

A complimentary, experimental approach to understanding locomotor hydrodynamics, however, now exists which involves direct measurement of fluid flow around swimming organisms (Stamhuis and Videler, 1995; Müller *et al.*, 1997; Drucker and Lauder, 1999; Lauder, 2000; Wilga and Lauder, 2000). Although gathering experimental data on wake flow behind live, swimming fishes can be technically challenging, such information permits the calculation of forces exerted by propulsive surfaces on the fluid and allows one to avoid simplifying assumptions about patterns of fin motion, as often required for theoretical modeling. Over the last several years a number of technical advances have facilitated the application of experimental hydrodynamic methods for studying locomotion in fishes, and have resulted in new insights into mechanisms of aquatic propulsion. In this paper we review a key new experimental approach to the study of locomotor hydrodynamics, digital particle image velocimetry (DPIV), and provide an overview of the significant functional insights into the biomechanics of swimming gained from recent DPIV studies. These insights are presented as ten "lessons learned" from experimental wake visualization that have general significance for the study of animal locomotion through fluids.

Functional Insights from Wake Visualization

The importance of understanding how propulsive surfaces of fishes effect motion of water and the significance of being able to quantify flow in the wake of propulsors has long been recognized (Gray, 1953; Webb, 1975), but the desire for wake visualization data has, until recently, not been matched by our technical ability to acquire such data. In a discussion of conflicting hypotheses of function proposed for fish fins, Harris (1938, p. 33) concluded that "many of the problems concerning the use of these . . . fins by the fishes can only be solved by a series of accurate and laborious hydrodynamical experiments." Writing in 1988, Webb noted (p. 710) that "ideally, momentum changes would be determined from direct observations of flow patterns or pressure fields around a swimming animal," but that "adequate techniques are rarely available to do this." More recently, in an analysis of the state of research on aquatic animal propulsion, Dickinson (1996, p. 553) argued similarly that in order to make significant progress we need to acquire "more elaborate flow visualizations and force measurements from swimming animals."

In an effort to obtain at least qualitative data on the wake of swimming fishes, researchers have employed a wide variety of approaches, including the tracking of streams of dye in the wake of the body and fins, and observing fish swimming in shallow layers of milk or in thermally stratified water so that disturbances in the fluid resulting from movement of the animal can be visualized (Rosen, 1959; Strickler, 1975; McCutchen, 1977; Ferry and Lauder, 1996). None of these approaches, however, provide the type of quantitative data needed to calculate locomotor forces and to understand the hydrodynamic significance of fin design.

Within the last five years biologists have begun to apply a technique originally developed for examining man-made flows in engineering applications: digital particle image velocimetry (DPIV) (Willert and Gharib, 1991; Krothapalli *et al.*, 1997; Raffel *et al.*, 1998; Stanislas *et al.*, 2000). The DPIV technique involves seeding a moving fluid with small reflective particles and using a powerful laser to illuminate a thin slice of this flow. The laser is focused using a series of lenses into a light sheet that is 1–2 mm thick and about 10 cm wide. Light scattered by the particles within the flow is imaged using a high-speed video recording system to provide a time series of images showing particle displacement. By performing a cross-correlation analysis (Willert and Gharib, 1991) to compare the pattern of particle images in consecutively recorded video fields, a two-dimensional matrix of velocity vectors can be calculated that describes the average magnitude and orientation of flow over the course of the video framing period Δt (typically 4–33 msec). High video frame rates are required to avoid out-of-plane loss of particle images over Δt. As opposed to tracking the movement of individual particles within the laser plane, DPIV analysis relies on changes in grayscale pixel intensity from one digitized video frame to the next to provide a uniform distribution of velocity vectors across the entire flow field. Further details of engineering aspects of this technique are available in Adrian (1991) and Raffel *et al.* (1998), and the application of DPIV to problems of fish locomotion is discussed in Anderson (1996), Müller *et al.* (1997), Drucker and Lauder (1999), Wilga and Lauder (1999), Wolfgang *et al.* (1999), and Lauder (2000).

For our research on the hydrodynamics of locomotion in fishes we have used the experimental arrangement diagrammed in Figure 1. Fish swim in the center of a recirculating flow tank with one or more fins intersecting the laser light sheet, thereby allowing visualization of the wake. A high-speed video camera (250 frames sec^{-1}) is used to image the pattern of particle movement within the light sheet (Fig. 1: Camera 1). A second synchronized camera provides a perpendicular reference view, monitoring the position of the fish relative to the light sheet via a small angled mirror in the flow (Fig. 1: Camera 2). Sample images of flow patterns in the wake, represented by matrices of velocity vectors calculated from DPIV analysis, are shown in Figure 2B. These velocity vectors provide the raw data needed for subsequent reconstruction of the three-dimensional geometry of the wake and calculation of both the orientation and magnitude of locomotor force as described below.

DPIV permits, for the first time, quantitative, empirical study of the wake of swimming fishes and, in spite of the relatively short time that such experimental data have been available, has resulted in significant

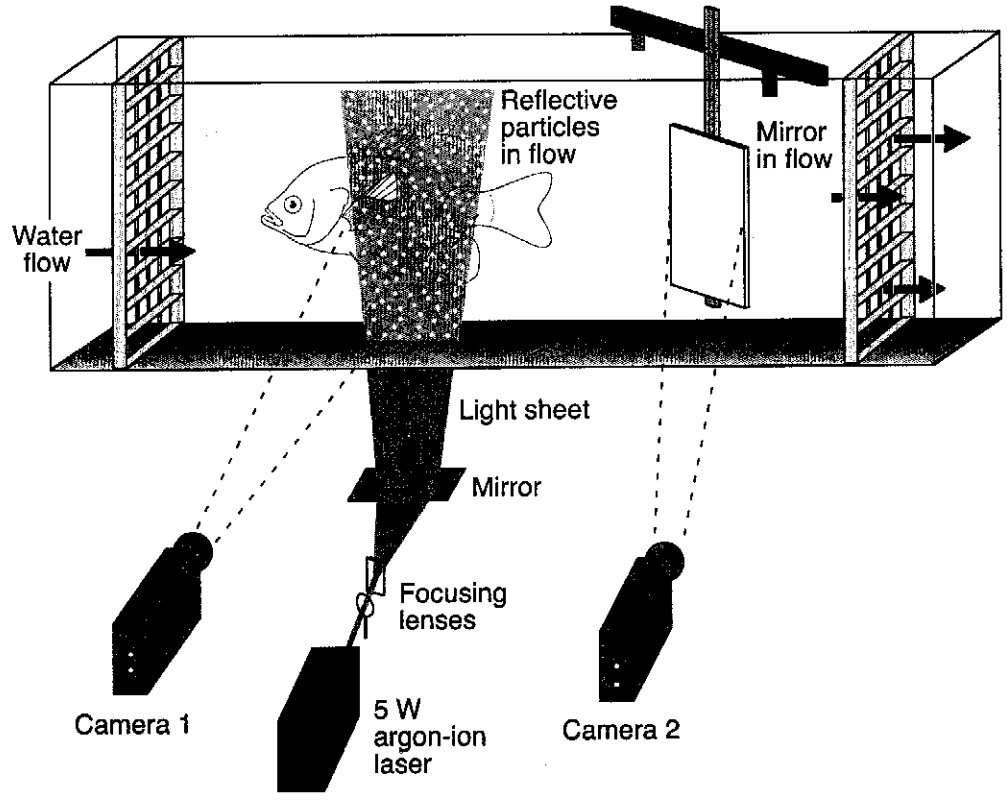

FIG. 1. Schematic illustration of the technique of digital particle image velocimetry (DPIV) as applied to the study of locomotion in fishes. Fish swim in the center of the working area of a recirculating flow tank (delimited by upstream and downstream collimator grids); water in the flow tank is seeded with near-neutrally buoyant, reflective particles (hollow silver-coated glass spheres, 12 μm mean diameter). Light from a continuous-wave argon-ion laser is focused into a sheet approximately 1–2 mm thick and 10 cm wide, and projected into the working area where this light is reflected by particles in the water. As fish swim, their fins break the plane of the light sheet and shed a wake into the water illuminated by the laser. Images of this water motion are recorded by a high-speed video camera (Camera 1). Simultaneous images of the fish in a perpendicular perspective are obtained from a second, synchronized video camera (Camera 2) which views the position of the fin within the laser light sheet via a small mirror located downstream at a 45-degree angle to the flow (exaggerated in size in this schematic figure). After Drucker and Lauder (1999).

new insights into the biomechanics of aquatic animal locomotion. Below we present ten major findings about the mechanisms of fish locomotion that have resulted from recent experimental hydrodynamic analyses. Some of these findings are primarily technical and reflect recent knowledge gained about how effectively to conduct DPIV analyses in fishes, while other functional insights take the form of new biological information about locomotor mechanics. The final point we present addresses the issue of hydrodynamics and evolution, and represents a broader level of analysis for future study.

1. Three-dimensional DPIV analysis is critical for reconstructing wake geometry

The DPIV technique can provide quantitative information about the velocity of water moving in the wake of a swimming animal. For any single orientation of the laser light sheet, a two-dimensional velocity field can be calculated that describes flow patterns in the vicinity of the propulsor. In analyzing wake structure, however, it is critical to reorient the light sheet in separate experiments so that it illuminates flow in perpendicular sections of the animal's wake (Fig. 2A). Representative flow fields for three orthogonal planes of analysis are given in Figure 2B. In this example, flow produced by the pectoral fin of a bluegill sunfish (*Lepomis macrochirus*) is shown during steady labriform locomotion. Study of flow in three dimensions is essential for reconstructing both the gross morphology of the wake as well as its spatial orientation with respect to the animal. The appearance of paired, counterrotating vortices in the wake of the pectoral fin (Fig. 2B) is reflected in plots of fluid vorticity, which provides a measure of local rotation within the flow fields (Fig. 2C). Analysis of the relative positions of paired vortices in perpendicular planes allows a schematic three-dimensional reconstruction of the pectoral fin wake. The patterns of Figure 2C are consistent with slices through an enclosed, toroidal vortex filament, or vortex ring. With each complete fin stroke, the pectoral fin of sunfish generates a single obliquely oriented vortex ring with a central region of jet flow (Fig. 2D). During slow swimming (0.5 body length sec^{-1}), vortex ring radius is approximately 2 cm in each of the three perpendicular planes of analysis, indicating a roughly symmetrical, near-circular loop. Vortices observed in transections of this loop are of comparable strength in

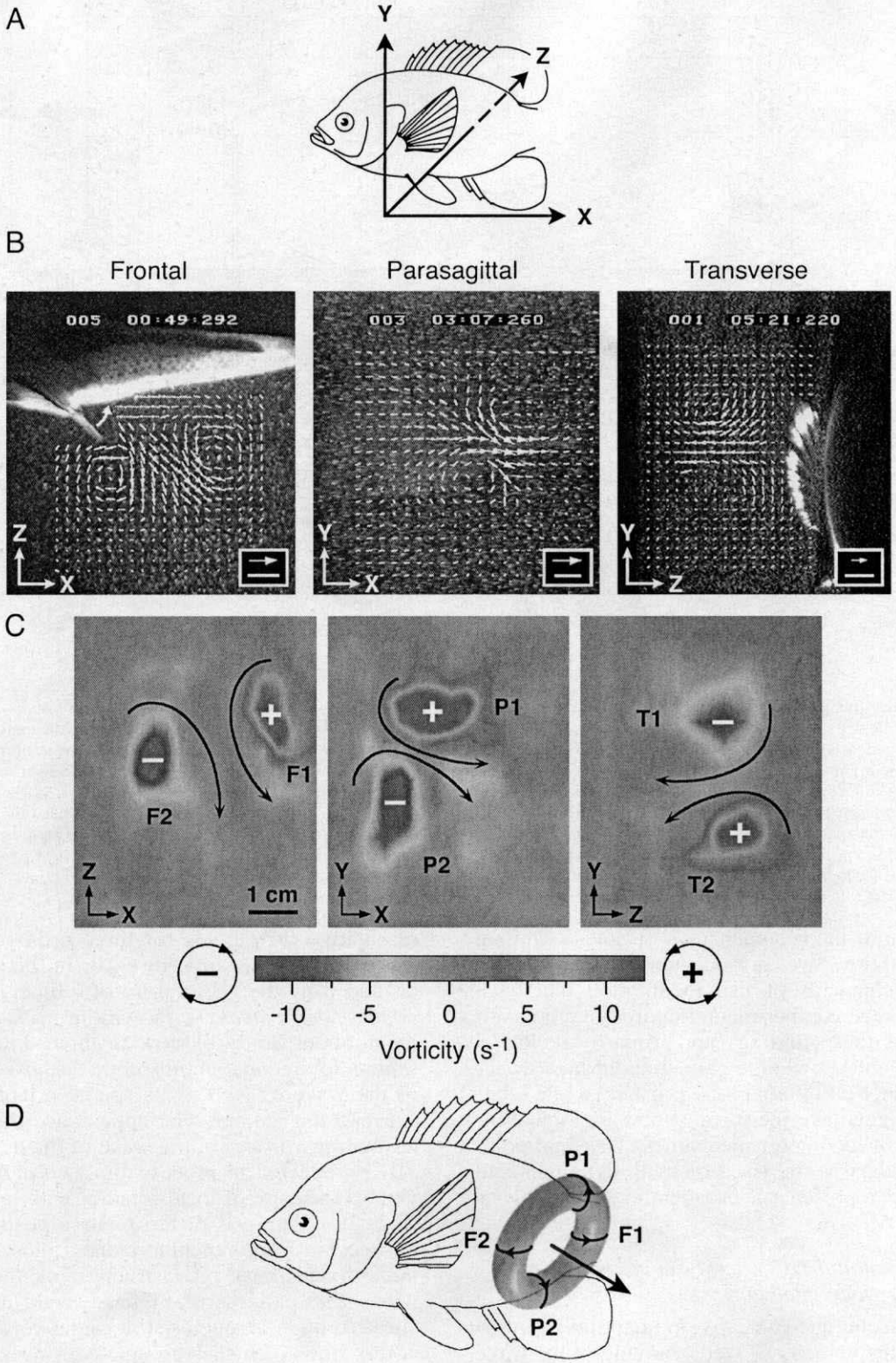

FIG. 2. Overview of experimental approach used to reconstruct the three-dimensional morphology of the wake of swimming fishes. A. By reorienting focusing lenses and mirrors (*cf.*, Fig. 1), laser light sheets may be arranged in three separate perpendicular planes: frontal (*XZ*), parasagittal (*XY*) and transverse (*YZ*). For each plane, flow velocity fields (B) and vorticity components (C) can be calculated. Based on such data in three dimensions, the geometry of large-scale structures in the wake can be determined. In the case illustrated, the pectoral fin stroke of bluegill sunfish swimming at 0.5 body length sec^{-1} produces paired counterrotating vortices in each plane (B) (curved arrow in frontal-plane image shows the direction of pectoral fin movement near the end of the upstroke; free-stream velocity from left to right has been subtracted from each vector matrix). Corresponding centers of vorticity are visible in each plane (C) (centers of counterclockwise and clockwise flow indicated by + and −, respectively). These vorticity patterns can be reconstructed as a single vortex ring, rotated laterally and inclined

each of the three planes. Specifically, average wake circulation does not differ significantly across planes (range = 43–61 g-cm sec^{-1}; one-way analysis of variance: df among planes = 2, df within planes = 7, $P = 0.65$), a result matching the theoretical expectation for a symmetrical vortex ring under Helmholtz's theorem (Fung, 1990).

2. DPIV analysis reveals the orientation of locomotor reaction forces

In certain specific cases, hypotheses of function can be tested by flow visualization in a single plane, and by an analysis of the direction of force application alone. One such case concerns the function of the heterocercal tail in fishes. Ray-finned fishes such as sturgeon possess a heterocercal tail morphology which is asymmetrical with respect to the horizontal axis: the dorsal lobe is longer than the ventral lobe and contains the caudal extension of the vertebral column. This caudal fin structure contrasts with the externally symmetrical homocercal morphology present in most teleost fishes such as bluegill sunfish (Lauder, 1989, 2000). One hypothesis current in the literature is that, as a result of their asymmetrical structure, heterocercal tails should generate a lift force posteriorly that induces a rotational moment around the center of mass of the body tending to pitch the head ventrally (Aleev, 1969). Liao and Lauder (2000) conducted a DPIV analysis to test this hypothesis in freely swimming ray-finned fish. The authors measured the orientation of fluid force produced by the tail in white sturgeon (*Acipenser transmontanus*) relative to the angle of the body during both steady horizontal locomotion and vertical maneuvering. Since locomotor forces directed laterally (*i.e.*, to the right and left) by steadily swimming fish cancel on average over the course of each stride, it was necessary only to resolve wake forces in the vertical (*XY*) plane. However, because sturgeon swim steadily with their body at a significant angle to the horizontal and because this angle changes during vertical maneuvering (Wilga and Lauder, 1999), it was essential to measure both body angle and wake jet orientation simultaneously in this *XY* plane in order to evaluate the rotational moments exerted by the heterocercal tail.

Plotting the orientation of the tail jet versus body angle for swimming sturgeon reveals two key features of heterocercal tail function (Fig. 3). First, during steady horizontal locomotion sturgeon maintain an average body angle of approximately 7° to the horizontal, and produce a vortex jet with an average inclination of −6°. This result indicates that during horizontal locomotion the reaction force acting on the sturgeon's heterocercal tail effectively intersects the center of mass of the body and therefore does not induce a substantial pitching moment as has been previously hypothesized (Aleev, 1969). Second, while rising and sinking in the water column, white sturgeon are capable of actively varying the direction of force produced by the tail through an angle of 10° on average. The slope of the jet angle–body angle relationship is significantly different from that of a hypothetical 180° line representing the condition in which heterocercal tail force is always directed opposite to the angle of the body (Fig. 3). Since the regression line intersects the 180° line, sturgeon must be adjusting the angle of the tail jet: tail force is directed at a greater angle than expected during locomotion at high body angles (*e.g.*, during rising in the water column), and at a lower angle than predicted when body angle is negative as during sinking behavior (Liao and Lauder, 2000).

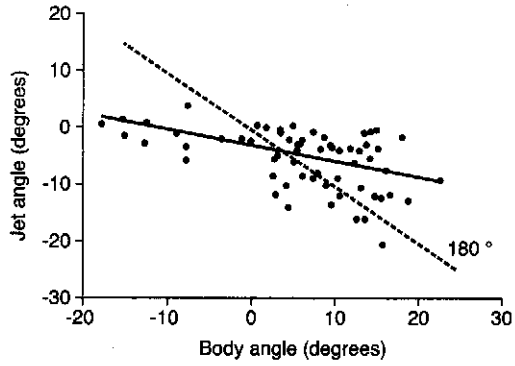

FIG. 3. Angle of the central fluid jet through vortex rings generated by the tail of white sturgeon plotted as a function of body angle during steady horizontal locomotion and vertical maneuvering at 1.2 body length sec^{-1}. Solid line indicates significant linear regression ($P < 0.001$; $N = 62$ tail beats). Vortex ring jet angle was measured from parasagittal-plane flow fields. Determining the orientation of the locomotor reaction force relative to body angle provides information about the force balance on swimming fishes. If the sturgeon tail functioned to generate force directly posteriorly (*i.e.*, parallel to the orientation of the body), data points would be expected to fall along the dashed line representing a constant angular deviation of 180°. Indeed, during steady swimming, the mean body angle (+7°) is effectively equal but opposite to the jet angle (−6°). However, these flow visualization measurements show that sturgeon can actively modulate the direction of force production with their tail during rising and sinking maneuvers: during swimming at high body angles, the jet angle is greater than expected, while at low body angles the jet angle is less than predicted. From Liao and Lauder (2000).

3. DPIV analysis allows calculation of the magnitude of locomotor forces

In addition to revealing the orientation of locomotor reaction forces, DPIV analysis can also provide quantitative information about the magnitude of forces ap-

←

relative to the horizontal, produced during each fin beat (D). In C and D, the labels F1–2, P1–2 and T1–2 indicate the centers of vorticity observed in each planar view of the wake. In D, curved arrows represent vortices observed in perpendicular laser light sheets and the straight arrow indicates the mean orientation of the fluid jet passing through the center of the vortex ring. Scales in B: arrow, 20 cm sec^{-1}; bar, 1 cm. Adapted from Drucker and Lauder (1999).

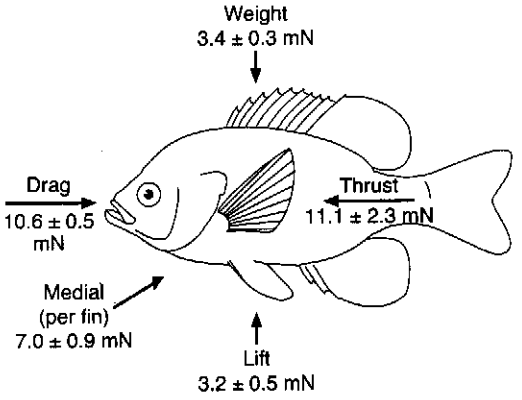

FIG. 4. Experimentally determined three-dimensional force balance on bluegill sunfish swimming with the pectoral fins alone at 0.5 body length (L) sec^{-1} (10.7 cm sec^{-1}). Reported thrust and lift values (mean ± SEM; N = 10, 12) were calculated from hydrodynamic data on vortex rings shed into the wake, and represent the mean reaction forces experienced by both the left and right pectoral fins together over the course of the fin-stroke period. Total body drag was measured directly by anesthetizing the same fish used in DPIV experiments and towing them individually from a force transducer within the flow tank at a current speed 0.5 L sec^{-1}. Observed differences between the measured thrust and drag forces are not statistically significant. Similarly, the stroke-averaged lift force calculated from vortex rings matches the body weight of sunfish under water. On opposite sides of the body, each pectoral fin experiences a relatively large medially directed reaction force, exceeding the per-fin thrust force by 25% on average. From Drucker and Lauder (1999).

plied to the fluid during swimming. Locomotor forces experienced by aquatic propulsors can be calculated as the reaction to the time rate of change in wake momentum (Milne-Thomson, 1966; Ellington, 1984; Dickinson and Götz, 1996). In our DPIV studies, the total stroke-averaged fluid force generated by a fish's fin is taken as the momentum of vortex ring structures shed into the wake divided by the time period over which the wake is produced (Drucker and Lauder, 1999, 2000, 2001*a*, *b*). Vortex ring momentum is estimated separately in each of the three perpendicular planes at the end of each fin stroke as the product of water density, mean circulation magnitude of paired vortices in midline sections of the ring, and the projected area of the vortex ring onto the plane of analysis. According to the average orientation of velocity vectors comprising the central fluid jet, the total force can be resolved into three perpendicular components: thrust, lift, and medially directed (parallel to the X, Y and Z reference axes, respectively; Fig. 2A).

The accuracy of DPIV in estimating wake forces is supported by an experimental analysis of the hydrodynamic force balance on freely swimming fish. Drucker and Lauder (1999) compared stroke-averaged forces calculated from DPIV wake measurements to empirically determined counter-forces during slow labriform swimming by bluegill sunfish. Lift and thrust forces derived from wake velocity fields were not significantly different from the resistive forces of body weight and total body drag, respectively (t-tests: df = 16, 18, P = 0.56, 0.73; Fig. 4). On opposite sides of the animal, medially directed forces on each pectoral fin arising in reaction to lateral wake force are presumed to balance, since sunfish show negligible sideslip during the course of the stroke cycle. Such a force equilibrium obviously matches the theoretical expectation for animals moving straight-ahead at constant speed, yet previous attempts to determine such a force balance experimentally have rarely been successful (see Spedding, 1987 for an exception). Empirically determining the force balance on a freely swimming fish indicates that DPIV can successfully detect the major vortical structures shed by swimming animals, and validates the technique for measuring locomotor forces from the wake.

4. Swimming speed can have a major impact on wake structure

Experimental studies of fluid flow generated by swimming fishes have revealed two factors having a consistent, important influence on the structure of the wake. The first of these is swimming speed. Figure 5

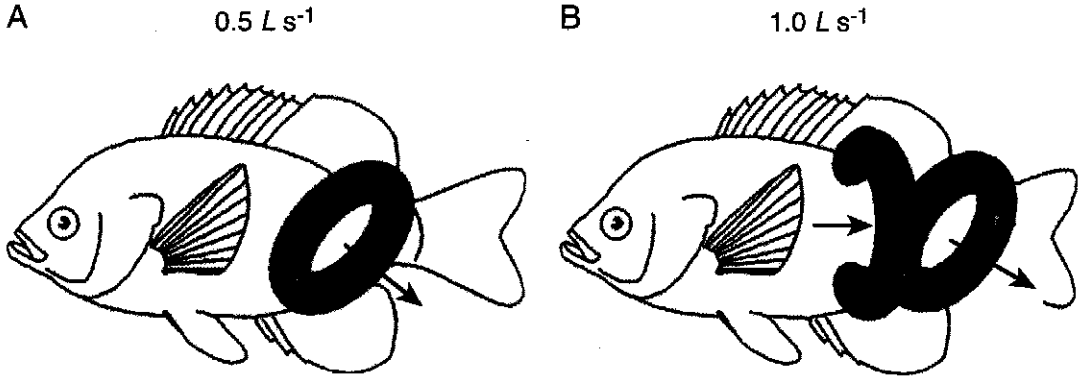

FIG. 5. Effect of swimming speed on the structure of the vortex wake in bluegill sunfish. A. At 0.5 body length (L) sec^{-1} (half of the maximal labriform swimming speed) the pectoral fin wake consists of a single vortex ring produced per fin beat cycle. B. At 1.0 L sec^{-1} (the maximal pectoral-fin swimming speed) the wake is composed of one complete vortex ring generated on the downstroke of the pectoral fin and a linked vortex filament produced by the upstroke, which terminates on the flank of the fish to form a second, incomplete ring attached to the body. In these schematic reconstructions of wake morphology, curved arrows represent centers of vorticity observed in perpendicular laser light sheets, and straight arrows indicate the direction of jet flow through the center of each vortex ring. Modified from Drucker and Lauder (1999).

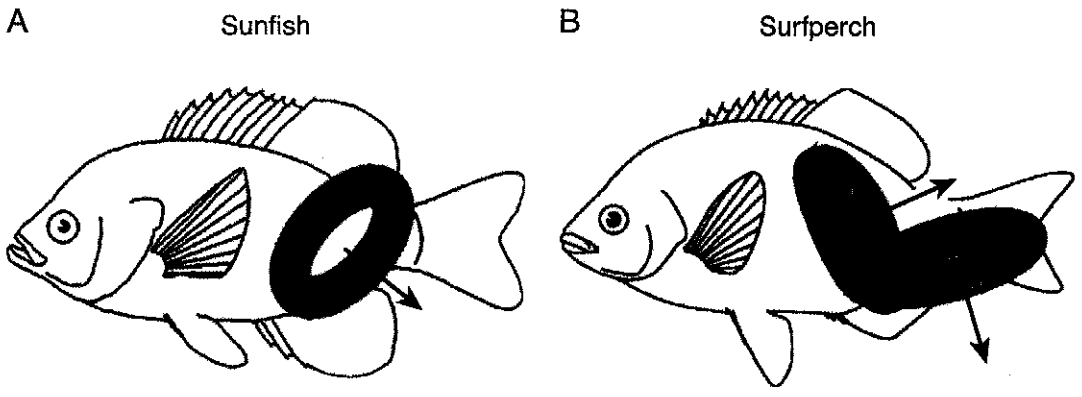

FIG. 6. Interspecific differences in the structure of the vortex wake in labriform swimmers. The pectoral fin wake of bluegill sunfish and black surfperch is shown with each fish at 50% of its respective maximal pectoral-fin swimming speed (*cf.*, Fig. 7). Sunfish generate a single, laterally oriented vortex ring during each stroke cycle (A), whereas surfperch shed paired vortex rings, each of which having a downstream-directed fluid jet (B). Curved arrows represent centers of vorticity observed in perpendicular planar sections of the wake, and straight arrows signify the direction of the jet through the center of each vortex ring. Modified from Drucker and Lauder (2000).

shows three-dimensional reconstructions of the pectoral fin wake of bluegill sunfish swimming at 50% and 100% of the maximum labriform swimming speed. The major difference in wake structure observed relates to the number of vortex rings shed during the stroke. At low speed each fin downstroke produces a single vortex ring (Fig. 5A), whereas at high speed both the downstroke and upstroke are hydrodynamically active, together resulting in a pair of linked vortex rings, each with a central fluid jet (Fig. 5B). The overall effect of swimming speed is to increase the size of the vortex wake, a pattern reflecting the injection of additional momentum into the fluid behind the animal. Such a momentum addition is necessary for swimming animals to match the increased drag forces experienced at higher speeds.

5. DPIV can reveal interspecific differences in vortex wake morphology

A second factor influencing wake morphology is related to taxonomic variation. Different fish species can show markedly different vortex wake structures, even when swimming at comparable speeds. Our interspecific DPIV studies compare wake dynamics of fishes swimming at equal fractions of their respective maximal swimming speeds within a gait. (The concept of the gait transition as representing an equivalent level of exercise for different swimming animals is reviewed by Drucker, 1996.) The wakes of two representative perciform teleost fishes, the bluegill sunfish and the black surfperch (*Embiotoca jacksoni*), are illustrated in Figure 6. At 50% of each species' top labriform swimming speed, vortex structures shed by the pectoral fin show clear variation. With each complete downstroke–upstroke cycle, the sunfish sheds a single ring, while the surfperch sheds two linked rings. Further, the sunfish's ring is rotated so that its central fluid jet has a large lateral component of velocity (Fig. 6A). In contrast, the surfperch generates rings oriented so that both the downstroke and upstroke jets have strong downstream components of velocity (Fig. 6B). Such differences in wake structure provide critical information for interpreting interspecific variation in swimming performance.

6. DPIV analysis can provide new insights into the limits to locomotor performance

Despite their close phylogenetic relationship and similar adult sizes and body shapes, sunfish and surfperch exhibit a pronounced difference in steady swimming ability. Comparably sized animals (*i.e.*, approximately 20 cm in total length L) show a two-fold difference in maximal labriform swimming speed. Sunfish exhibit a pectoral-to-caudal-fin gait transition speed (U_{p-c}) of 1.0 L sec^{-1}, whereas surfperch can swim twice as fast as with the pectoral fins before recruiting the caudal fin to augment thrust. For both species, thrust calculated from the pectoral fin wake plateaus at U_{p-c} as axial undulation begins, but surfperch are able to generate significantly greater wake force than sunfish at high swimming speed (Fig. 7). Underlying this interspecific difference in speed and thrust may be physiological variation between the two species, including differences in cardiovascular, respiratory or muscular performance.

However, DPIV analysis reveals that there is an additional important hydrodynamic factor that may help explain the upper limit of pectoral-fin swimming speed. Observed interspecific variation in the orientation of the wake jet (*e.g.*, Fig. 6) becomes increasingly pronounced as swimming speed increases. Figure 8 depicts the mean orientation of jet flow associated with vortex rings produced by sunfish and surfperch at swimming speeds up to and above U_{p-c}. In surfperch, the average downstroke jet angle, as measured in the horizontal plane, decreases with speed from 67° to 1° on average, indicating an increasing contribution of the pectoral fins to forward thrust. Surfperch, in other words, can redirect their vortex jet increasingly downstream as swimming speed increases (Fig. 8). In contrast, sunfish progressively reorient this jet laterally. The downstroke jet angle in sunfish shows an unex-

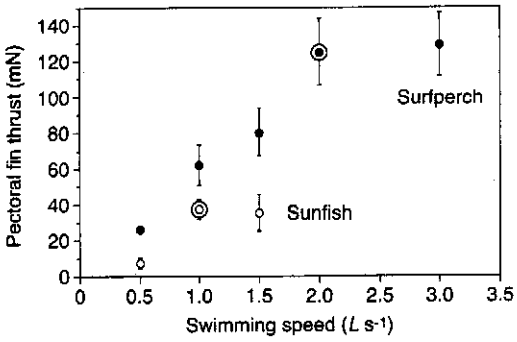

FIG. 7. Pectoral fin thrust calculated from wake flow data for sunfish and surfperch plotted as a function of swimming speed in body lengths L traveled per second. Data are shown as mean ± SEM (N = 3–6 fin beats) and represent average forward thrust generated by both pectoral fins together over the stride period. The maximal labriform swimming speed for each species is circled. Note that pectoral fin thrust reaches a plateau for sunfish at 1.0 L sec^{-1} while the comparable plateau for surfperch begins at 2.0 L sec^{-1}. At speeds greater than 1.0 L sec^{-1} sunfish recruit the caudal and dorsal fins to supplement pectoral fin thrust. Modified from Drucker and Lauder (2000).

pected increase with swimming speed to nearly a 90-degree angle to the body, reflecting the production of a large lateral component of force and a proportional reduction in thrust (Fig. 8). We conclude that swimming performance, as measured by maximal swimming speed within a gait (*e.g.*, Fig. 7), may be limited by a species' ability to direct wake momentum downstream. With wake flow oriented essentially perpendicular to the axis of progression, as in sunfish nearing top speed, no variation in pectoral fin shape or increase in pectoral muscle power output can raise the observed speed limit.

7. DPIV demonstrates the functional versatility of fish fins

Insights into locomotor mechanisms provided by DPIV analysis are not limited to steady swimming behavior. The technique can also provide valuable information about the mechanics of unsteady maneuvering, a behavior likely comprising the largest portion of a swimming animal's locomotor time budget (Fuiman and Webb, 1988; Webb, 1991; Boisclair and Tang, 1993; Krohn and Boisclair, 1994). Investigation of the wakes of fish performing a range of swimming tasks has exposed the breadth of the locomotor repertoire of fish fins—propulsors whose great functional versatility was not apparent from analyses of steady swimming alone.

In studies of steady swimming, the plateauing of thrust from the pectoral fins at the gait transition (Fig. 7) suggested a potential upper limit to the rate at which these fins can add momentum to the wake. However, study of maneuvering in the same species has revealed that steady swimming forces do not accurately represent the pectoral fin's complete range of function. Drucker and Lauder (2001*b*) compared wake dynamics

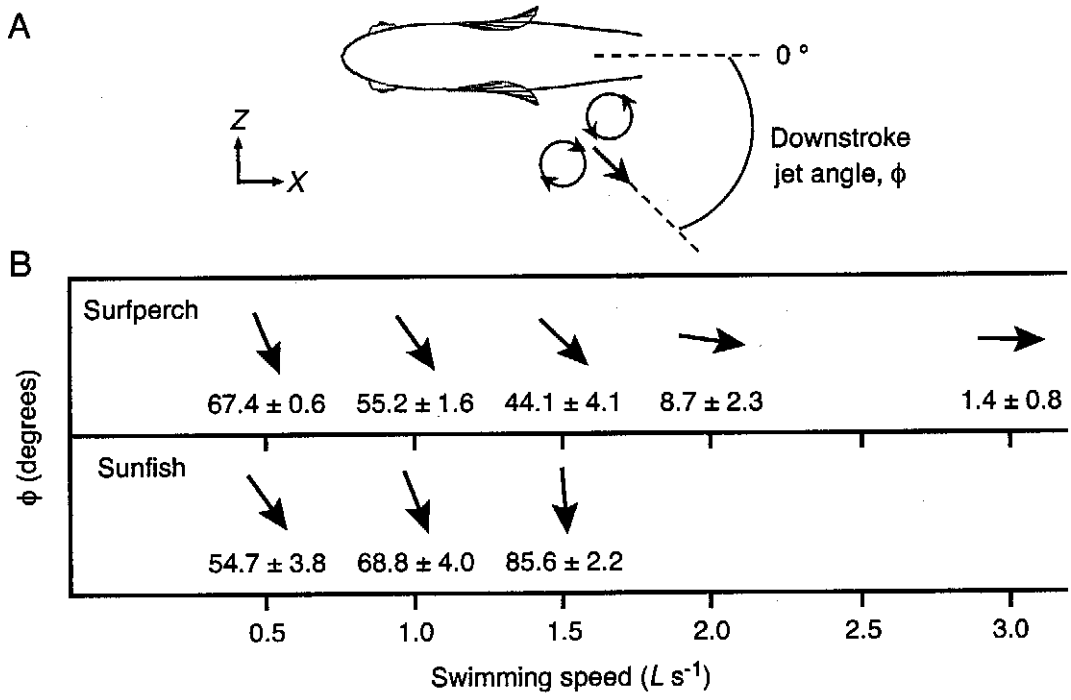

FIG. 8. Orientation of the fluid jet passing through the center of pectoral-fin vortex rings over a range of swimming speeds in bluegill sunfish and black surfperch. A. Downstroke jet angle (ϕ), as measured in the frontal (XZ) plane, is defined as 0° when velocity vectors within the jet are oriented on average directly downstream. Positive values for this angle reflect a lateral component of velocity within the jet. B. For both species, mean ϕ (reported with SEM; N = 3–8 fin beats) is represented by the orientation of black arrows. With increasing swimming speed, the wake jet of surfperch rotates into a more downstream orientation providing increased thrust. In sunfish, the jet is progressively reoriented laterally as swimming speed increases, limiting the thrust available to overcome drag. L, total body length. From Drucker and Lauder (2000).

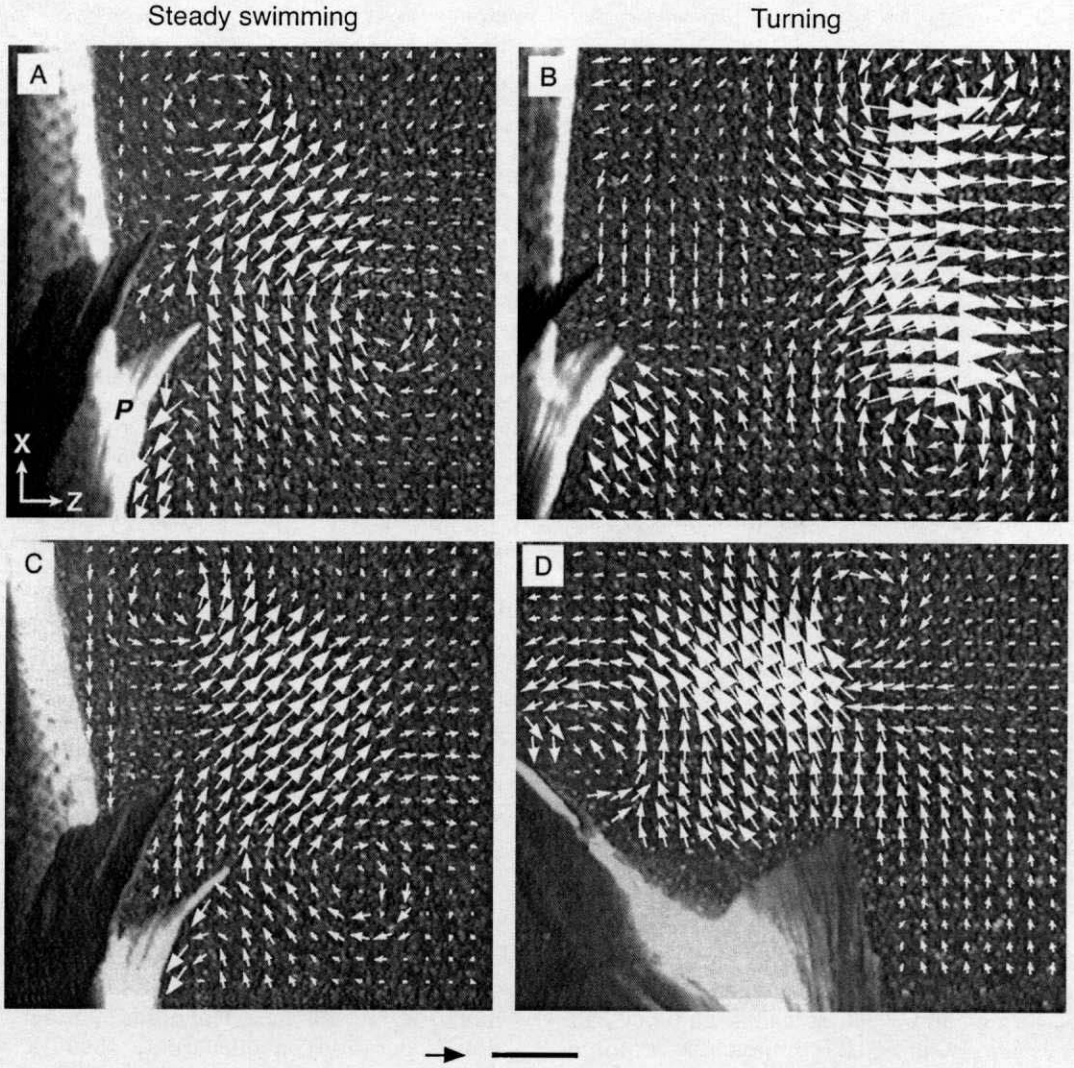

FIG. 9. Wake flow patterns in the frontal (*XZ*) plane during steady labriform locomotion and pectoral-fin turning maneuvers in bluegill sunfish. Water velocity fields are shown at the final stage of the upstroke of the pectoral fin (labeled *P*). Free-stream velocity of 0.5 body length (*L*) sec^{-1} (11.2 cm sec^{-1}) has been subtracted from the *X*-component of each velocity vector to reveal vortical wake structures. A. Pattern of fluid flow in the wake of the pectoral fin during steady swimming at 0.5 *L* sec^{-1}. B. Wake flow produced by the pectoral fin during turning elicited by a stimulus issued from the right. This pectoral fin beat cycle immediately follows the steady fin beat illustrated in A. As this strong-side wake develops, with a laterally directed fluid jet, the body rotates in the opposite direction to the left. C. Pattern of fluid flow during a separate, steady pectoral fin beat. D. Turning wake generated subsequent to the fin beat in C in response to a stimulus issued from the left. This weak-side wake arises on the upstroke and contains jet flow oriented nearly parallel to the body axis. The reaction to this momentum flow causes the fish to translate upstream (toward the bottom of the page) away from the source of the stimulus. Scales: arrow, 10 cm sec^{-1}; bar, 1 cm. From Drucker and Lauder (2001*b*).

during steady swimming and turning in bluegill sunfish. Fish performing rectilinear labriform locomotion were exposed to a visual and auditory stimulus, which induced an evasive maneuver involving both pectoral fins. Unlike "fast-start" escape turning driven by Mauthner-cell-mediated body flexion (Eaton *et al.*, 1977, 1988; Eaton and DiDomenico, 1986), pectoral fin turning is a relatively slow behavior, involving an initial body rotation (up to 32 degrees sec^{-1}) and a subsequent period of body translation (2–8 cm sec^{-1}).

Examples of velocity fields in the wake of the pectoral fin during steady swimming and turning behavior are given in Figure 9. As observed previously for sunfish (Drucker and Lauder, 1999, 2000), planar visualizations of the pectoral fin wake generated during steady swimming reveal paired counterrotating vortices with central fluid jets (Fig. 9A, C). Subsequent turning results in a dramatic reorganization of wake structure. For the pectoral fin closer to the stimulus (termed the "strong-side" fin), each downstroke–upstroke cycle results in vortices that are considerably larger and stronger than those generated during steady swimming. In addition, the wake jet has a predominantly lateral, rather than downstream, orientation (Fig. 9B). The wake of the contralateral, or "weak-side," fin is also radically reoriented such that the

TABLE 1. *Kinematic and hydrodynamic measurements from steady pectoral fin swimming and turning by bluegill sunfish.*

Measurement	Steady swimming	Turning: strong side	Ratio	Steady swimming	Turning: weak side	Ratio
Duration of propulsive fin movement (ms)	996 ± 46	565 ± 51	0.57*	1,034 ± 88	208 ± 21	0.20*
Mean jet angle (degrees)	41.2 ± 3.9	91.6 ± 5.5	2.22*	45.8 ± 6.8	0.3 ± 4.5	0.01*
Mean jet velocity (cm s^{-1})	7.6 ± 0.6	13.9 ± 2.1	1.83*	8.0 ± 0.6	11.4 ± 1.2	1.42*
Force, lateral component (mN)	5.4 ± 0.4	20.9 ± 6.5	3.83*	5.3 ± 0.8	−5.3† ± 4.4	1.00*
Force, posterior component (mN)	4.7 ± 0.6	2.1 ± 1.3	0.44*	5.6 ± 1.5	48.3 ± 5.5	8.64*
Force ratio, lateral : posterior	1.18 ± 0.09	10.05 ± 4.15	—	1.11 ± 0.29	0.11 ± 0.03	—

All measurements are tabulated as mean ± SEM (N = 9 pectoral fin beats per behavior performed by four individuals; data from Drucker and Lauder, 2001*b*). Wake measurements are from frontal-plane velocity fields and are reported for the end of the upstroke.

Jet angle is measured relative to longitudinal body axis (Fig. 8A). Wake forces are stroke-averaged measurements reported per fin.

Ratio, absolute value of the measurement for turning expressed as a proportion of that for steady swimming.

Measurements for steady swimming at 0.5 body length s^{-1} and for subsequent turning were compared statistically using paired t-tests (df = 8). Asterisks indicate significant differences at the Bonferroni-adjusted α = 0.008.

† Negative value indicates a force that is oriented medially, on average, relative to the longitudinal axis of the fish at the onset of propulsive fin movement.

thrust jet falls roughly in line with the longitudinal axis of the body at the onset of body translation (Fig. 9D).

The impressive functional versatility of the pectoral fin is revealed through quantification of fin kinematics and wake dynamics during steady swimming and turning. Turning involves pectoral fin motions that are significantly shorter in duration than those observed during steady swimming (by up to a factor of five, Table 1). While the vortex ring's jet remains at nearly a 45-degree angle to the body on average during steady swimming (Table 1, Fig. 9A, C), momentum flows during turning are redirected by up to 50° (Table 1, Fig. 9B, D). During turning, the strong-side pectoral fin generates a wake jet whose average velocity is approximately twice as great as that produced during steady swimming (Table 1). In addition, the magnitude of wake force varies significantly between the two behaviors. The strong- and weak-side fins generate laterally and posteriorly directed components of force during turning that exceed those produced during rectilinear locomotion by 4- and 9-fold, respectively. Furthermore, the ratio of lateral to posterior force measured for the two behaviors spans almost two orders of magnitude (Table 1). These results emphasize the importance of examining a range of locomotor behaviors when defining the hydrodynamic repertoire of aquatic animal propulsors. Continued quantitative analysis of the wake of teleost fishes will improve our understanding of how fins serve different functions in the face of different locomotor demands.

8. DPIV reveals hydrodynamic force partitioning among fins

In addition to being functionally versatile, fish fins are highly integrated components of the propulsive system. Fishes can employ multiple fins distributed over the body simultaneously both to produce and modulate swimming force. Three fins in particular are observed to work together in a coordinated way during swimming: the pectoral fin, the caudal fin and the dorsal fin (*e.g.,* Arreola and Westneat, 1996). For perciform fishes, the pectoral fin and tail are known to play important roles in propulsion and there is now a substantial literature on the function of these fins (*e.g.,* Bainbridge, 1958; Aleev, 1969; Webb, 1973, 1975; Blake, 1979, 1983; Geerlink, 1983; Videler, 1993; Gibb *et al.*, 1994; Drucker and Jensen, 1996; Lauder and Jayne, 1996; Walker and Westneat, 1997; Lauder, 2000). Functions traditionally assigned to the dorsal fin of perchlike fishes, however, have been mostly non-propulsive. For example, during steady swimming the dorsal fin has been described as a keel or body stabilizer (Aleev, 1969). During turning, the dorsal fin has been hypothesized to serve as a pivot point, again playing a largely passive, non-propulsive role (Helfman *et al.*, 1997, p. 168).

DPIV can be used to test explicitly whether simultaneously recruited fish fins play active roles in generating propulsive force. Figure 10 illustrates two possible vortex flow patterns behind bodies within moving fluid. At intermediate Reynolds numbers (*i.e.,* before flow separation), a bluff body sheds a trail of staggered, counterrotating vortices. Flow between each pair of vortices has a component of velocity oriented upstream, thereby reducing the momentum of the incident flow (Fig. 10A). This flow pattern is known as a von Kármán street and is a classic example of a *drag-producing wake*. In contrast, a heaving and pitching foil, like a fish's fin, can produce vortices with opposite rotation, so that a downstream-directed fluid jet is generated between each vortex pair (Fig. 10B). This is an actively produced *thrust wake*, or reverse von Kármán street (von Kármán and Burgess, 1935; Weihs, 1972*b*; Lighthill, 1975; Triantafyllou *et al.*, 1993, 2000), which adds momentum to the fluid behind the fin.

Analysis of the wake of sunfish during high-speed swimming reveals that the trailing edge of the dorsal fin clearly plays an active role in propulsion. At a steady swimming speed of 1.1 L sec^{-1} (*i.e.,* slightly above U_{p-c} for 20 cm-long fish), the soft dorsal fin is observed to undulate regularly and shed a reverse von Kármán street (Drucker and Lauder, 2001*a*). Thus, at this speed, the dorsal fin supplements the thrust produced by the oscillating pectoral and caudal fins. The total thrust generated by all fins over the course of

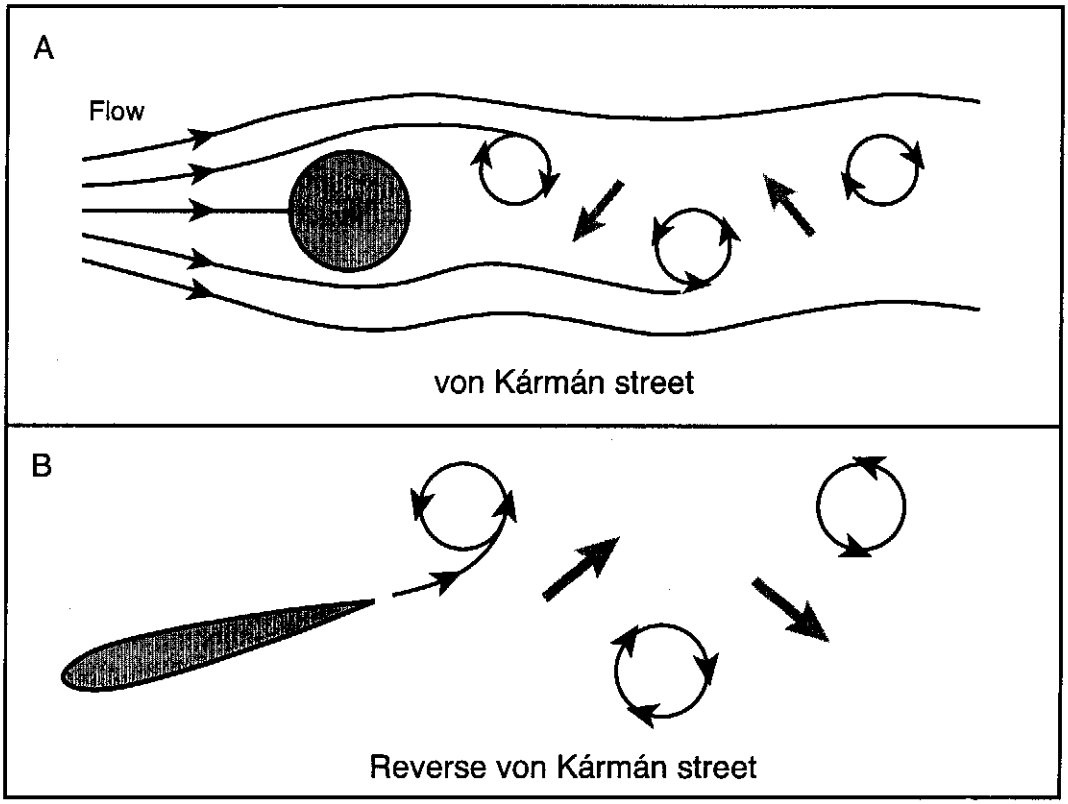

FIG. 10. Comparison of theoretically expected patterns of wake flow behind a stationary cylinder (A) and a heaving and pitching foil (B). Incident fluid flow in both panels is from left to right. The bluff body in A generates a drag wake composed of staggered counterrotating vortices with interspersed jet flow (gray arrows) oriented upstream (*i.e.*, a von Kármán street). As the streamlined foil in B oscillates it also leaves a staggered wake of vortices, but because the sense of vortex rotation is opposite to that shown in A this wake is termed a reverse von Kármán street. This actively generated wake produces jet flow between alternating vortex pairs that is oriented downstream. In reaction to these momentum jets, forward thrust is exerted on the foil.

each stride is partitioned among the three fin systems as shown in Figure 11A; note that the soft dorsal fin contributes 12% of total thrust on average. During slow turning maneuvers in sunfish (described above), the soft dorsal fin is also active, shedding a laterally oriented momentum jet at the end of the body-rotation phase (Drucker and Lauder, 2001*a*). Both the pectoral and dorsal fins, therefore, exert laterally oriented wake forces during this unsteady swimming behavior, with the dorsal fin generating an average of 35% of the total (Fig. 11B). The fact that the soft dorsal fin produces approximately 10% of the total thrust generated by all fins during steady swimming, and more than one-third of the total lateral force during turning, underlines its active role in propulsion. The partitioning of swimming force among multiple fins is likely a widespread characteristic of the teleost locomotor system, but as yet has received very little experimental study.

9. DPIV shows that wake interaction among fins may enhance thrust production

The observation that more than one fin can shed a vortex wake at the same time suggests the possibility of hydrodynamic interaction among nearby propulsors. Theoretical studies of fish locomotion have emphasized the potential for wake interaction among fish fins to increase propulsive efficiency (Lighthill, 1970; Wu, 1971; Yates, 1983; Weihs, 1989). Experimental work in non-biological systems has demonstrated that vortex trails shed by upstream bodies can intercept and affect the strength of developing vortices generated by bodies downstream. Specifically, it has been shown that the drag wake of an upstream bluff body can interact in either a constructive or destructive way with the near-field thrust wake produced by a downstream oscillating foil (Gopalkrishnan *et al.*, 1994; Anderson, 1996; Triantafyllou *et al.*, 2000). The type of interaction observed depends on the sign of vortex rotation and the encounter phase of the foil with respect to the upstream vortices. For two adjacent foils shedding a thrust wake, as in a swimming fish, annihilation or reinforcement of vorticity will also depend on encounter kinematics.

Using DPIV, Drucker and Lauder (2001*a*) examined the dynamics of wake interaction between the soft dorsal fin and tail of bluegill sunfish. Given the proximity of these fins (see Fig. 11A), both constructive and destructive interactions among wake vortices are theoretically possible. During steady swimming slightly above the gait transition speed (1.1 L sec^{-1}), both fins exhibit a sinusoidal pattern of motion with a mean phase lag of 120 msec. A horizontal laser light sheet

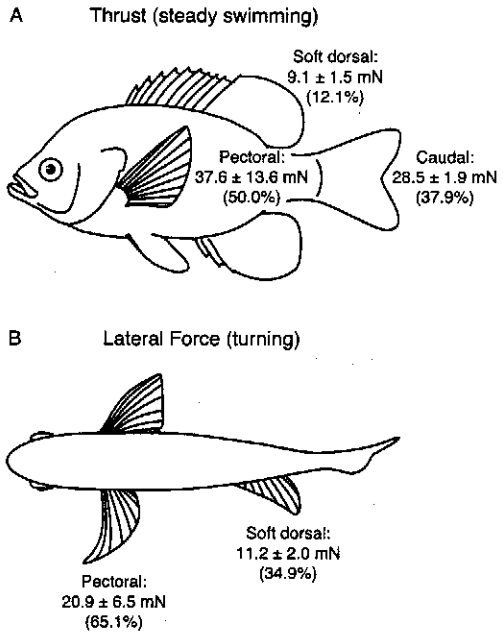

FIG. 11. Summary of the components of wake force contributed by different fins of bluegill sunfish during steady swimming and turning behavior. All forces are stroke-averaged and reported as mean ± SEM (N = 6–11 fin beats). For each behavior, the percentage of total force generated by each fin is given in parentheses. A. Thrust generated during steady swimming at 1.1 body length sec^{-1} by the soft dorsal fin, tail and both pectoral fins together (per complete stroke cycle). B. Laterally oriented force produced by the strong-side pectoral fin during the early stage of a turning maneuver (*cf.*, Fig. 9B) and by the soft dorsal fin during the latter stage of the turn. The partitioning of force among fins in A and B underlines the ability of teleost fishes to use multiple propulsors simultaneously and independently during locomotion. The observed contribution of the soft dorsal fin to locomotor force (12% of thrust; 35% of lateral force) supports an active role of this fin in propulsion for perciform fishes. Force data from Drucker and Lauder (1999, 2001*a*, *b*).

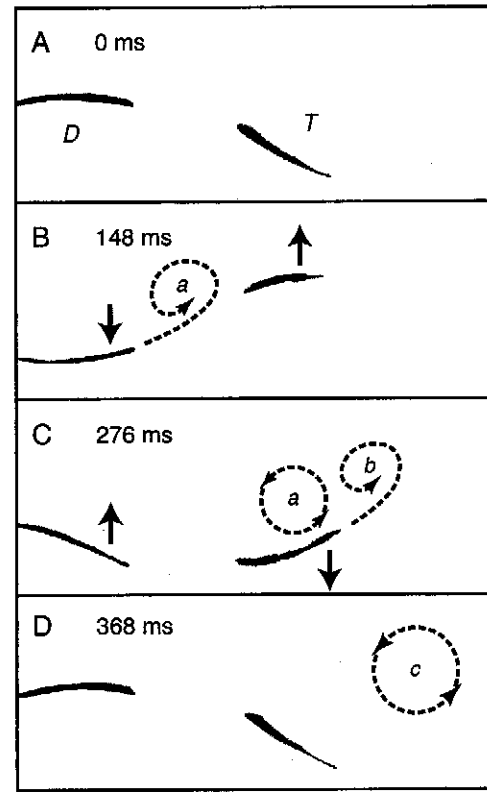

FIG. 12. Interaction between vortices generated by the soft dorsal fin (D) and the dorsal lobe of the tail (T) proposed to enhance thrust production by fishes. Dorsal-view silhouettes of the fins in bluegill sunfish are shown in images from a high-speed video sequence of steady locomotion at 1.1 body length sec^{-1}. DPIV wake visualization within a horizontal plane intersecting both fins reveals vortices (represented schematically by dashed lines) that are produced during the course of the stroke cycle. The direction of fin movement is indicated by solid-line arrows. Vortex a is shed as the soft dorsal fin sweeps laterally (A–B) and migrates downstream during the development of an analogous tail vortex b (C). As the tail completes its stroke, the two counterclockwise-rotating vortices merge, forming a single larger downstream vortex c (D). The process illustrated in A–D is repeated on both sides of the body to yield the tail's reverse von Kármán street wake (*cf.*, Fig. 10B). Reinforcement of developing circulation around the tail through interception of the dorsal fin's vortices is proposed as a mechanism for enhancing thrust. Modified from Drucker and Lauder (2001*a*).

was used to illuminate simultaneously the ventral portion of the soft dorsal fin and the dorsal lobe of the tail. Within this plane, the tail undergoes a lateral excursion 0.5 cm greater on average than that of the trailing edge of the dorsal fin, such that at the extremes of its left–right motion, the tail moves into the immediate vicinity of vortices cast by the soft dorsal fin.

Patterns of movement of the two fins and vortex shedding during the stroke cycle are illustrated in Figure 12. As the soft dorsal fin undulates laterally, it produces a trailing vortex (Fig. 12: vortex a) which represents part of the fin's reverse von Kármán street (*cf.*, Fig. 10B). The DPIV video record reveals that the dorsal fin's vortex moves downstream and is consistently intercepted by the dorsal lobe of the tail. Vortex a is observed to follow the surface of the tail while the tail itself develops bound vorticity, which is ultimately shed as a distinct vortex (Fig. 12: vortex b). The two analogous vortices have the same rotational sense and correct timing of interaction to merge constructively immediately downstream of the tail, forming a larger, combined vortex (Fig. 12: vortex c). We hypothesize that, in the early stage of the tail's half-stroke, the presence of rotational flow from the dorsal fin's wake (vortex a) increases incident velocity over the tail and enhances same-sign vorticity bound to the tail (flow that enters the wake as vortex b). Such reinforcement of developing circulation is proposed as a mechanism for directing additional energy into the tail's wake and for increasing thrust production by the tail.

10. Experimental hydrodynamic analysis can provide insight into the functional significance of evolutionary variation in fin design

To date, the focus of experimental hydrodynamic analyses of fish locomotion has been on the detailed mechanics of propulsor function as reflected in the functional insights presented above. However, new

biomechanical tools such as DPIV can also be applied to examine the evolution of locomotor function over a broad phylogenetic scale. The fins of fishes have undergone a number of major historical transformations in design, yet, until now, we have not been equipped with an experimental technique for understanding the functional consequences of these evolutionary trends.

One example of such evolutionary variation in fin structure, long-recognized by vertebrate anatomists, is the suite of structural transformations that have occurred in pectoral fin morphology within ray-finned fishes (Schmalhausen, 1916; Breder, 1926; Harris, 1937, 1938; Greenwood *et al.*, 1966; Gosline, 1971; Alexander, 1974; Rosen, 1982; Webb, 1982). In this group, clear trends exist in two aspects of fin design: anatomical position and fin base orientation. Basal taxa typically exhibit pectoral fins positioned low on the side of the body with horizontally inclined fin bases (*e.g.*, sturgeon and gar). More derived taxa commonly possess fins located higher on the body, near the center of mass of the animal, with more vertically oriented insertions (*e.g.*, perciform fishes). (Within the ray-finned fishes, there are, as expected, scattered exceptions to these anatomical trends. Among basal taxa, for instance, *Polypterus* exhibits nearly vertically inclined pectoral fins; among perciforms, some labroid fishes show more horizontal fin bases.) At present, the functional significance of these general patterns of evolutionary variation is poorly understood. One implication of these trends in pectoral fin design is that numerous differences may exist between basal and derived clades in the function of the fins during locomotion. For example, it is likely that the angle of inclination of the pectoral fin base constrains the range of directions in which force may be applied on the fluid during swimming. Specifically, taxa possessing horizontally inclined pectoral fins, with limited anteroposterior mobility, are expected to generate relatively low laterally directed force, as compared to taxa with more vertically inclined fin bases. In addition, fishes with ventrally positioned pectoral fins may exert greater rotational moments around the center of mass of the body than species with mid-dorsally positioned fins. In general, the observed variation in pectoral fin anatomy among ray-finned fishes is predicted to influence (a) the capacity for generating stabilizing and propulsive forces, (b) the balance of fluid forces acting on the body during steady swimming, and (c) the generation of pitching and yawing moments during unsteady maneuvering. Until recently, functional predictions of this kind could not be tested experimentally, as the tools for measuring the crucial data—locomotor force magnitudes and orientations—were not available. The use of experimental hydrodynamic methods, including quantitative wake visualization, will allow much-needed clarification of the functional significance of evolutionary trends in fin design in fishes.

CONCLUSIONS

The combination of traditional biomechanical tools, including kinematic analysis, measurement of muscle activity, and analysis of muscle fiber power output, with new experimental approaches such as digital particle image velocimetry promises a more integrated understanding of the mechanics of organismal motion through fluids. By combining data on muscle physiology and internal force production with patterns of propulsor movement and measurement of the forces exerted externally on the fluid, we will in future work be well-equipped to address long-standing questions about the mechanics and evolution of locomotion in aquatic animals.

ACKNOWLEDGMENTS

Discussions with Erik Anderson, Jamie Anderson, Ellen Freund, Jon Posner, Eric Tytell and Danny Weihs provided many insights into wake dynamics and the mechanisms of fish locomotion. Collaborative research conducted with Jimmy Liao, Jen Nauen and Cheryl Wilga was instrumental in formulating the ideas presented in this paper. We thank Mark Westneat and an anonymous reviewer for constructive criticisms of the manuscript. The research described herein and the preparation of this manuscript was supported by NSF grants DBI-9750321, IBN-9807012 and IBN-0090896 to E.G.D. and G.V.L.

REFERENCES

Adrian, R. J. 1991. Particle imaging techniques for experimental fluid mechanics. Ann. Rev. Fluid Mech. 20:421–485.

Aleev, Y. G. 1969. *Function and gross morphology in fish.* Translated from the Russian by M. Raveh. Keter Press, Jerusalem.

Alexander, R. McN. 1974. *Functional design in fishes*, 3rd ed. Hutchinson and Co., London.

Altringham, J. D. and I. A. Johnston. 1990. Modelling muscle power output in a swimming fish. J. Exp. Biol. 148:395–402.

Anderson, J. 1996. Vorticity control for efficient propulsion. Ph.D Diss. MIT/WHOI, 96-02.

Arreola, V. I. and M. W. Westneat. 1996. Mechanics of propulsion by multiple fins: Kinematics of aquatic locomotion in the burrfish (*Chilomycterus schoepfi*). Proc. R. Soc. Lond. B 263:1689–1696.

Bainbridge, R. 1958. The speed of swimming of fish as related to size and to the frequency and amplitude of the tail beat. J. Exp. Biol. 35:109–133.

Biewener, A. A. and R. J. Full. 1992. Force platform and kinematic analysis. *In* A. A. Biewener (ed.), *Biomechanics: Structures and systems*, pp. 45–73. Oxford University Press, Oxford.

Blake, R. W. 1979. The mechanics of labriform locomotion. I. Labriform locomotion in the angelfish (*Pterophyllum eimekei*): An analysis of the power stroke. J. Exp. Biol. 82:255–271.

Blake, R. W. 1981. Influence of pectoral fin shape on thrust and drag in labriform locomotion. J. Zool. London 194:53–66.

Blake, R. W. 1983. *Fish locomotion.* Cambridge University Press, Cambridge.

Boisclair, D. and M. Tang. 1993. Empirical analysis of the influence of swimming pattern on the net energetic cost of swimming in fishes. J. Fish Biol. 42:169–183.

Breder, C. M., Jr. 1926. The locomotion of fishes. Zoologica (New York) 4:159–296.

Carling, J., T. L. Williams, and G. Bowtell. 1998. Self-propelled anguilliform swimming: Simultaneous solution of the two-dimensional Navier-Stokes equations and Newton's laws of motion. J. Exp. Biol. 201:3143–3166.

Cavagna, G. A. 1975. Force platforms as ergometers. J. Appl. Physiol. 39:174–179.

Coughlin, D. J. 2000. Power production during steady swimming in largemouth bass and rainbow trout. J. Exp. Biol. 203:617–629.

Dickinson, M. H. 1996. Unsteady mechanisms of force generation in aquatic and aerial locomotion. Amer. Zool. 36:537–554.

Dickinson, M. H. and K. G. Götz. 1996. The wake dynamics and flight forces of the fruit fly *Drosophila melanogaster*. J. Exp. Biol. 199:2085–2104.

Domenici, P. and R. W. Blake. 1997. The kinematics and performance of fish fast-start swimming. J. Exp. Biol. 200:1165–1178.

Drucker, E. G. 1996. The use of gait transition speed in comparative studies of fish locomotion. Amer. Zool. 36:555–566.

Drucker, E. G. and J. S. Jensen. 1996. Pectoral fin locomotion in the striped surfperch. I. Kinematic effects of swimming speed and body size. J. Exp. Biol. 199:2235–2242.

Drucker, E. G. and G. V. Lauder. 1999. Locomotor forces on a swimming fish: Three-dimensional vortex wake dynamics quantified using digital particle image velocimetry. J. Exp. Biol. 202: 2393–2412.

Drucker, E. G. and G. V. Lauder. 2000. A hydrodynamic analysis of fish swimming speed: Wake structure and locomotor force in slow and fast labriform swimmers. J. Exp. Biol. 203:2379–2393.

Drucker, E. G. and G. V. Lauder. 2001*a*. Locomotor function of the dorsal fin in teleost fishes: Experimental analysis of wake forces in sunfish. J. Exp. Biol. 204:2943–2958.

Drucker, E. G. and G. V. Lauder. 2001*b*. Wake dynamics and fluid forces of turning maneuvers in sunfish. J. Exp. Biol. 204:431–442.

Eaton, R. C., R. A. Bombardieri, and D. Meyer. 1977. The Mauthner initiated startle response in teleost fish. J. Exp. Biol. 66:65–81.

Eaton, R. C. and R. DiDomenico. 1986. Role of the teleost escape response during development. Trans. Amer. Fish. Soc. 115:128–142.

Eaton, R. C., R. DiDomenico, and J. Nissanov. 1988. Flexible body dynamics of the goldfish C-start: Implications for reticulospinal command mechanisms. J. Neurosci. 8:2758–2768.

Ellington, C. P. 1984. The aerodynamics of hovering insect flight. IV. Aerodynamic mechanisms. Phil. Trans. R. Soc. London B 305:79–113.

Fauci, L. J. 1996. A computational model of the fluid dynamics of undulatory and flagellar swimming. Amer. Zool. 36:599–607.

Ferry, L. A. and G. V. Lauder. 1996. Heterocercal tail function in leopard sharks: A three-dimensional kinematic analysis of two models. J. Exp. Biol. 199:2253–2268.

Fish, F. E. 1998. Comparative kinematics and hydrodynamics of odontocete cetaceans: Morphological and ecological correlates with swimming performance. J. Exp. Biol. 201:2867–2877.

Fuiman, L. A. and P. W. Webb. 1988. Ontogeny of routine swimming activity and performance in zebra danios (Teleostei: Cyprinidae). Anim. Behav. 36:250–261.

Fung, Y. C. 1990. *Biomechanics: Motion, flow, stress, and growth*. Springer-Verlag, New York.

Geerlink, P. J. 1983. Pectoral fin kinematics of *Coris formosa* (Teleostei, Labridae). Neth. J. Zool. 33:515–531.

Gibb, A. C., B. C. Jayne, and G. V. Lauder. 1994. Kinematics of pectoral fin locomotion in the bluegill sunfish *Lepomis macrochirus*. J. Exp. Biol. 189:133–161.

Gillis, G. B. 1996. Undulatory locomotion in elongate aquatic vertebrates: Anguilliform swimming since Sir James Gray. Amer. Zool. 36:656–665.

Gopalkrishnan, R., M. S. Triantafyllou, G. S. Triantafyllou, and D. Barrett. 1994. Active vorticity control in a shear flow using a flapping foil. J. Fluid Mech. 274:1–21.

Gosline, W. A. 1971. *Functional morphology and classification of teleostean fishes*. University of Hawaii Press, Honolulu.

Gray, J. 1953. The locomotion of fishes. *In* S. M. Marshall and A. P. Orr (eds.), *Essays in marine biology*, pp. 1–16. Oliver and Boyd, Edinburgh.

Greenwood, P. H., D. E. Rosen, S. H. Weitzman, and G. S. Myers. 1966. Phyletic studies of teleostean fishes, with a provisional classification of living forms. Bull. Amer. Mus. Nat. Hist. 131: 343–455.

Grillner, S. and P. Wallen. 1984. How does the lamprey central nervous system make the lamprey swim? J. Exp. Biol. 112:337–357.

Harris, J. E. 1937. The mechanical significance of the position and movements of the paired fins in the Teleostei. Pap. Tortugas Lab. 31:173–189.

Harris, J. E. 1938. The role of the fins in the equilibrium of the swimming fish. II. The role of the pelvic fins. J. Exp. Biol. 16: 32–47.

Helfman, G. S., B. B. Collette, and D. E. Facey. 1997. *The diversity of fishes*. Blackwell Science, Malden, Massachusetts.

Jayne, B. C. and G. V. Lauder. 1995. Are muscle fibers within fish myotomes activated synchronously? Patterns of recruitment within deep myomeric musculature during swimming in largemouth bass. J. Exp. Biol. 198:805–815.

Krohn, M. M. and D. Boisclair. 1994. Use of a stereo-video system to estimate the energy expenditure of free-swimming fish. Can. J. Fish. Aquat. Sci. 51:1119–1127.

Krothapalli, A., L. Lourenco, and C. Shih. 1997. Visualization of velocity and vorticity fields. *In* Y. Nakayama and Y. Tanida (eds.), *Atlas of visualization III*, pp. 69–82. CRC Press, Boca Raton.

Lauder, G. V. 1989. Caudal fin locomotion in ray-finned fishes: Historical and functional analyses. Amer. Zool. 29:85–102.

Lauder, G. V. 2000. Function of the caudal fin during locomotion in fishes: Kinematics, flow visualization, and evolutionary patterns. Amer. Zool. 40:101–122.

Lauder, G. V. and B. C. Jayne. 1996. Pectoral fin locomotion in fishes: Testing drag-based models using three-dimensional kinematics. Amer. Zool. 36:567–581.

Liao, J. and G. V. Lauder. 2000. Function of the heterocercal tail in white sturgeon: Flow visualization during steady swimming and vertical maneuvering. J. Exp. Biol. 203:3585–3594.

Lighthill, J. and R. Blake. 1990. Biofluiddynamics of balistiform and gymnotiform locomotion. Part 1. Biological background and analysis by elongated-body theory. J. Fluid Mech. 212:183–207.

Lighthill, M. J. 1970. Aquatic animal propulsion of high hydromechanical efficiency. J. Fluid Mech. 44:265–301.

Lighthill, M. J. 1975. *Mathematical biofluiddynamics*. Society for Industrial and Applied Mathematics, Philadelphia.

Liu, H., R. J. Wassersug, and K. Kawachi. 1997. The three-dimensional hydrodynamics of tadpole locomotion. J. Exp. Biol. 200: 2807–2819.

Long, J. H., D. A. Pabst, W. R. Shepherd, and W. A. McLellan. 1997. Locomotor design of dolphin vertebral columns: Bending mechanics and morphology of *Delphinus delphis*. J. Exp. Biol. 200:65–81.

Luiker, E. A. and E. D. Stevens. 1993. Effect of stimulus train duration and cycle frequency on the capacity to do work in pectoral fin muscle of the pumpkinseed sunfish, *Lepomis gibbosus*. Can. J. Zool. 71:2185–2189.

McCutchen, C. W. 1977. Froude propulsive efficiency of a small fish, measured by wake visualization. *In* T. J. Pedley (ed.), *Scale effects in animal locomotion*, pp. 339–363. Academic Press, London.

Milne-Thomson, L. M. 1966. *Theoretical aerodynamics*, 4th ed. Macmillan, New York.

Müller, U. K., B. L. E. Van den Heuvel, E. J. Stamhuis, and J. J. Videler. 1997. Fish foot prints: Morphology and energetics of the wake behind a continuously swimming mullet (*Chelon labrosus* Risso). J. Exp. Biol. 200:2893–2906.

Raffel, M., C. E. Willert, and J. Kompenhans. 1998. *Particle image velocimetry: A practical guide*. Springer-Verlag, Heidelberg.

Roberts, T., R. Kram, P. Weyand, and C. R. Taylor. 1998. Energetics of bipedal running. I. Metabolic cost of generating force. J. Exp. Biol. 201:2745–2751.

Rome, L. C., D. Swank, and D. Corda. 1993. How fish power swimming. Science 261:340–343.

Rosen, D. E. 1982. Teleostean interrelationships, morphological function, and evolutionary inference. Amer. Zool. 22:261–273.

Rosen, M. W. 1959. Water flow about a swimming fish. Naval Ordnance Test Station Technical Paper 2298:1–96.

Schmalhausen, I. 1916. On the functions of the fins of the fish. Rev. Zool. Russe (Moscow) 1:185–214.

Spedding, G. R. 1987. The wake of a kestrel (*Falco tinnunculus*) in flapping flight. J. Exp. Biol. 127:59–78.

Stamhuis, E. J. and J. J. Videler. 1995. Quantitative flow analysis around aquatic animals using laser sheet particle image velocimetry. J. Exp. Biol. 198:283–294.

Stanislas, M., J. Kompenhans, and J. Westerweel (eds.). 2000. *Particle image velocimetry: Progress towards industrial application.* Kluwer Academic Publishers, Dordrecht.

Strickler, J. R. 1975. Swimming of planktonic *Cyclops* species (Copepoda, Crustacea): Pattern, movements and their control. *In* T. Y. Wu, C. J. Brokaw, and C. Brennen (eds.), *Swimming and flying in nature*, Vol. 2, pp. 599–613. Plenum Press, New York.

Triantafyllou, G. S., M. S. Triantafyllou, and M. A. Grosenbaugh. 1993. Optimal thrust development in oscillating foils with application to fish propulsion. J. Fluids Struct. 7:205–224.

Triantafyllou, M. S., G. S. Triantafyllou, and D. K. P. Yue. 2000. Hydrodynamics of fishlike swimming. Annu. Rev. Fluid Mech. 32:33–53.

Videler, J. J. 1993. *Fish swimming*. Chapman and Hall, New York.

von Kármán, T. and J. Burgess. 1935. General aerodynamic theory—perfect fluids. *In* W. Durand (ed.), *Aerodynamic theory*, Vol. 2, pp. 346–349. Springer-Verlag, Berlin.

Walker, J. A. and M. W. Westneat. 1997. Labriform propulsion in fishes: Kinematics of flapping aquatic flight in the bird wrasse *Gomphosus varius* (Labridae). J. Exp. Biol. 200:1549–1569.

Walker, J. A. and M. W. Westneat. 2000. Mechanical performance of aquatic rowing and flying. Proc. R. Soc. London B 267: 1875–1881.

Wardle, C. S., J. J. Videler, and J. D. Altringham. 1995. Tuning in to fish swimming waves: Body form, swimming mode and muscle function. J. Exp. Biol. 198:1629–1636.

Webb, P. W. 1973. Kinematics of pectoral fin propulsion in *Cymatogaster aggregata*. J. Exp. Biol. 59:697–710.

Webb, P. W. 1975. Hydrodynamics and energetics of fish propulsion. Bull. Fish. Res. Bd Can. 190:1–159.

Webb, P. W. 1982. Locomotor patterns in the evolution of actinopterygian fishes. Amer. Zool. 22:329–342.

Webb, P. W. 1988. Simple physical principles and vertebrate aquatic locomotion. Amer. Zool. 28:709–725.

Webb, P. W. 1991. Composition and mechanics of routine swimming of rainbow trout, *Oncorhynchus mykiss*. Can. J. Fish. Aquat. Sci. 48:583–590.

Weihs, D. 1972*a*. A hydrodynamic analysis of fish turning manoeuvres. Proc. R. Soc. London B 182:59–72.

Weihs, D. 1972*b*. Semi-infinite vortex trails, and their relation to oscillating airfoils. J. Fluid Mech. 54:679–690.

Weihs, D. 1989. Design features and mechanics of axial locomotion in fish. Amer. Zool. 29:151–160.

Westneat, M. W. and J. A. Walker. 1997. Motor patterns of labriform locomotion: Kinematic and electromyographic analysis of pectoral fin swimming in the labrid fish *Gomphosus varius*. J. Exp. Biol. 200:1881–1893.

Wilga, C. D. and G. V. Lauder. 1999. Locomotion in sturgeon: Function of the pectoral fins. J. Exp. Biol. 202:2413–2432.

Wilga, C. D. and G. V. Lauder. 2000. Three-dimensional kinematics and wake structure of the pectoral fins during locomotion in leopard sharks, *Triakis semifasciata*. J. Exp. Biol. 203:2261–2278.

Willert, C. E. and M. Gharib. 1991. Digital particle image velocimetry. Exp. Fluids 10:181–193.

Wolfgang, M. J., J. M. Anderson, M. Grosenbaugh, D. Yue, and M. Triantafyllou. 1999. Near-body flow dynamics in swimming fish. J. Exp. Biol. 202:2303–2327.

Wu, T. Y. 1971. Hydromechanics of swimming propulsion. Part 3. Swimming and optimum movements of slender fish with side fins. J. Fluid Mech. 46:545–568.

Yates, G. T. 1983. Hydromechanics of body and caudal fin propulsion. *In* P. W. Webb and D. Weihs (eds.), *Fish biomechanics*, pp. 177–213. Praeger, New York.